Astron. Astrophys. 195, 230–244 (1988)

ASTRONOMY AND ASTROPHYSICS

The SMC compact blob N 81: a detailed multi-wavelength investigation *

M. Heydari-Malayeri **, T. Le Bertre, and P. Magain**

European Southern Observatory, Casilla 19001, Santiago 19, Chile

Received July 10, accepted September 18, 1987

Summary. This paper is devoted to an extensive investigation of the compact Small Magellanic Cloud H II region N81. Several observational techniques with various telescopes at ESO have been employed to acquire a multi-aspect view of the physical characteristics of this interesting nebula: CCD, IDS and Reticon high, medium and low resolution spectroscopy (range 3700–10000 Å), CCD imaging using 17 different filters, optical and infrared photometry at *UBVRI* and *JHK*. We also use the H I emission observations reported in the literature.

The nebula N81 is probably excited by one star of about 60 $M_\odot$ ($T_{\rm eff} = 47500$ K) accompanied by a cluster of about 10 B0 stars ($M = 15\,M_\odot$, $T_{\rm eff} = 32000$ K). We derive the absolute visual magnitude of the exciting star to be -5.1, corresponding to a bolometric magnitude of $M_{\rm bol} = -9.1$ and a luminosity of $3.5\ 10^5\ L_\odot$.

This nebula is a young H II region. From the equivalent width of the Hβ emission line we derive an age of $2.5\ 10^6$ yr for N81. We stress the importance of correcting the continuum emission around Hβ for the nebular contribution.

We derive the gas electron density and temperature and compute the chemical abundances of He, O, N, Ne, S, and Ar. The results are compared with the mean values available for the SMC.

The high resolution profile of N81 at Hβ was decomposed into its various components. We find the most probable three dimensional turbulent velocity in N81 to be about 3 km s^{-1}. We observationally confirm the proposition by Koornneef and Israel (1985) that the H_2 emission may be produced by the action of a mild shock moving through the ambient cloud of this nebula.

Interestingly, unlike other representatives of this category of H II regions in the Magellanic Clouds, N81 is not affected by the local dust.

The nebula N81 is associated with the SMC H I cloud of radial velocity +167 km s^{-1}, observed by McGee and Newton (1981). The neighboring H II complexes N83 are associated with a density peak of this H I cloud. N 88 A, another SMC H II blob, lying in the vicinity of N 81, is associated with another H I cloud. We speculate that N 81 and N 88 A may have been formed due to a collision between these two clouds.

Key words: Small Magellanic Cloud – interstellar medium – H II regions – compact H II blobs – O stars – abundances – excitation – high resolution velocity profile – CCD spectroscopy and imaging – optical and infrared photometry

1. Introduction

N 81 (Henize, 1956) situated in the wing of the Small Magellanic Cloud (SMC), south-east of the main bar, is an interesting nebula from several respects related to the problem of star formation in the SMC (other designations: Lindsay 481, IC 1644, DEM 138, and Nail 136).

Its very high surface brightness, absolute magnitude and compactness make this H II blob an almost unique object in the SMC. The only object rivaling it is N 88 (Testor and Pakull, 1985). Interstingly, these peculiar blobs, which should be very young H II regions, both lie in the same part of the SMC, where a very high percentage of stars (90%) are O-B2 supergiants and there are no F-G stars (Azzopardi, 1981).

Henize and Westerlung (1963) were the first to draw attention to this object. The chemical composition of N 81 was studied by Dufour and Killen (1977), Dufour and Harlow (1977; hereafter DH) and Dufour et al. (1982) using optical and UV spectroscopy. Koornneef and Israel (1985), carrying out two-micron near infrared spectrophotometry, detected molecular hydrogen associated with N 81.

The purpose of the present paper is to investigate several aspects of this H II blob in much more detail, using several observational techniques in a coordinated manner. We have for the first time obtained an almost complete set of CCD frames in various wavelengths, allowing investigation of the morphology and structure of this object. Obtaining several CCD, IDS, and Reticon spectra, we cover a wide range (3700–10000 Å) of the spectrum of N 81. Adding these data to the results of our optical and near infrared photometry, we can try to acquire a detailed knowledge of the physical properties of this object and to study its stellar content.

This work is a part of the investigation of excited H II blobs which we detected in the Magellanic Clouds (Heydari-Malayeri and Testor, 1982, 1983, 1985, 1986; Testor and Pakull, 1985). The knowledge of these regions and their exciting sources is essential for better understanding the history and mechanism of star

Send offprint requests to: M. Heydari-Malayeri

* Based on observations made at the European Southern Observatory

** On leave from DEMIRM, Observatoire de Paris, Section de Meudon

Table 1. Journal of the spectrographic observations

Grat. (Å mm^{-1}) (1)	Detector (2)	Range (Å) (3)	FWHM (Å) (4)	Slit dir. (5)	Size (″) (6)	Expo. (min) (7)	Date (8)
58	CCD	3889– 4764	3	EW	2	15	86 Jun. 17
58	CCD	3889– 4764	3	EW	2	20	86 Jun. 18
58	CCD	3889– 4764	3	EW	2	25	86 Jun. 19
114	CCD	5040– 6750	4.5	EW	2	10	87 Mar. 25
172	CCD	4300– 6800	12	EW	2	1	86 Jun. 21
172	CCD	4300– 6800	12	EW	2	2	86 Jun. 21
172	CCD	4300– 6800	12	NS	4	1	86 Jul. 22
172	CCD	4300– 6800	12	EW	4	1	86 Jul. 22
172	CCD	4300– 6800	12	EW	4	2	86 Jul. 22
172	CCD	4300– 6800	12	EW	4	5	86 Jul. 22
172	CCD	4300– 6800	12	EW	4	10	86 Jul. 22
172	IDS	3700– 6800	12	–	4×4	30	84 Dec. 12
450	Reticon	4000–10000	40	–	4×10	60	86 Sep. 30

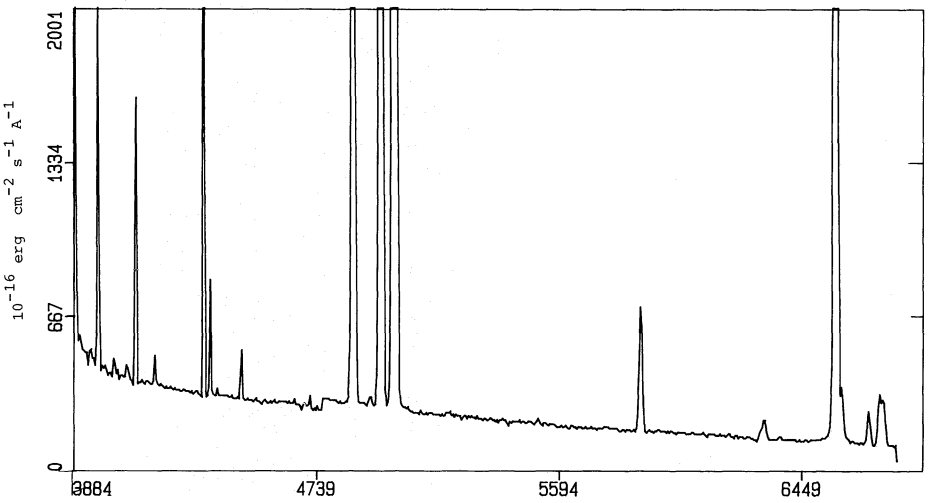

Fig. 1. A CCD spectrum of N 81. This is a composite of two spectra, one in the blue (effective resolution: 3 Å) and the other in the red (effective resolution: 12 Å). The effect at ~4739 Å is due to the matching procedure

formation in the Magellanic Clouds. We are gathering a homogeneous set of data on these regions. Reliable models of star formation require high quality data on these young constituents of the interstellar medium in the Magellanic Clouds.

This paper is arranged as follows: Section 2 presents the observations obtained with various instrumentations. Section 3 deals with morphology and brightness of N 81. Section 4 is devoted to temperature and density and Sect. 5 to the chemical abundances in N 81. Section 6 addresses the velocity structure of N 81 through studying the Hβ profile obtained with high resolution spectroscopy. Section 7 deals with excitation, ionizing sources, optical continuum properties, mass, equivalent width of the Hβ line, etc. In Sect. 8 we investigate the extinction properties of N 81 and in Sect. 9 we present the concluding remarks.

2. Observations and data reduction

2.1. Spectroscopy

2.1.1. CCD

Boller and Chivens spectrographs attached to the 2.20 m and 1.52 m telescopes at La Silla, were used to obtain long-slit spectra of N 81. The detector was a thinned backside illuminated RCA CCD chip; at the 2.20 m telescope a SID 501 EX, 512 × 320 pixels each pixel 30 μm × 30 μm (corresponding to 0″.35 on the sky in the direction of dispersion) and at the 1.52 m a high resolution chip SID 503, 1024 × 640 pixels, each pixel 15 μm × 15 μm. Table 1 gives more information about the CCD spectra (obtained in the first order). The first column indicates the dispersion of the spectrograph used. Column 2 presents the detector and column 3 the spectral range. The full widths at half maximums of the lines in each range are indicated in column 4. Columns 5 and 6 give the slit directions and widths for the CCD spectra. The aperture sizes for the IDS and Reticon are listed in column 6. Exposure times and observation dates are indicated in columns 7 and 8. Figure 1 displays and example of the CCD spectra obtained.

2.1.2. IDS and Reticon

The Image Dissector Scanner (IDS) and the Reticon were used with the Boller and Chivens spectrograph at the ESO 1.52 m telescope to obtain aperture spectra of N 81 in the first order. The Reticon is a complement to the IDS and allows obtention of

Table 2. Line intensities

λ	Iden.	F_λ	Error	I_λ	Note
3727, 29	[O II]	115.74	B	124.55	
3798	H 10	5.74	E	6.14	
3835	H 9]	8.06	E	8.60	
3869	[Ne III]	38.31	A	40.74	
3889, 90	H 8 + He I	27.57	B	29.27	
3934	I.S. Ca II				ab
3968, 70	[Ne III] + H 7	35.02	B	36.96	
4026	He I	2.73	C	2.87	
4068	[S II]	1.03	D	1.08	
4076	[S II]	1.04	D	1.09	
4102	Hδ	29.62	A	30.96	
4200	He II				ab
4341	Hγ	54.65	A	56.23	
4363	[O III]	8.35	A	8.58	
4388	He I	0.70	D	0.72	
4472	He I	4.42	A	4.51	
4541	He II				ab
4686	He II				ab
4711, 13	[Ar IV] + He I	1.05	B	1.06	
4740	[Ar IV]	0.49	C	0.49	
4861	Hβ	100.0	A	100.0	
4922	He I	1.02	C	1.02	
4959 + 5007	[O III]	698.86	A	694.11	
5198 + 5200	[N I]	0.42	C	0.41	
5270	[Fe III]	0.28	D	0.27	
5412	He II				ab
5518	[Cl III]	0.50	C	0.49	
5538	[Cl III]	0.34	C	0.33	
5755	[N II]	0.12	E	0.12	
5876	He I	11.43	A	10.99	
5896	I.S. Na I				ab
6300	[O I]	0.67	C	0.64	
6312	[S III]	2.01	C	1.91	
6364	[O I]	0.34	C	0.32	
6563	Hα	305.33	A	287.45	
6583, 48	[N II]	6.11	B	5.75	
6678	He I	3.32	A	3.12	
6717	[S II]	4.86	B	4.56	
6731	[S II]	4.55	B	4.26	
7065	He I	3.22	C	2.99	
7136	[Ar III]	11.54	B	10.70	
7319, 30	[O II]	5.19	B	4.79	
7751	[Ar III]	2.85	C	2.61	
9069	[S III]	16.40	B	14.65	
9229	P 9	3.90	D	3.48	
9532	[S III]	9.23	C	8.19	

$\log I(\mathrm{H}\beta) = -10.75 \pm 0.10\ \mathrm{erg\,cm^{-2}\,s^{-1}}$
$c(\mathrm{H}\beta) = 0.09 \pm 0.04$

spectra in the far red. See Table 1 for the characteristics of the spectra.

The CCD, IDS and Reticon data after being flat-fielded were corrected for the atmospheric extinction and for the detector response and calibrated in flux by observing several standard stars. The various spectra were combined into a composite spectrum covering from 3700 to 10000 Å. This was not a difficult task as the common lines in each range gave the same flux within about 10% accuracy.

The atmospheric dispersion was no problem for any of our spectrophotometric measurements. We checked the linearity of the spectra using the [O III] 5007/4959 intensity ratio, the theoretical value of which is 2.96 (Osterbrock, 1974). We checked this ratio for two kinds of spectra: those representing the total emission

Table 3. Log of the CCD images

Filter	λ (Å)	$\Delta\lambda$ (Å)	Expo. (s)	Tel.	Date
U	3560	510	20	3.60	85 Nov. 19
[O II]	3727, 29	10	1800	1.54	85 Dec. 13
B	4350	1000	3	3.60	85 Nov. 19
B	4350	1000	120	1.54	86 Jun. 23
He II	4686	10	300	1.54	85 Dec. 13
No. 1402	4794	68	300	1.54	85 Dec. 13
Hβ	4861	10	1800	1.54	85 Dec. 13
[O III]	5007	10	600	1.54	85 Dec. 13
V	5550	1000	1	3.60	85 Nov. 19
V	5550	1000	60	1.54	86 Jun. 23
V	5550	1000	120	1.54	86 Jun. 23
R	6500	1640	60	1.54	86 Jun. 23
Cont.	6646	78	300	1.54	86 Jun. 23
Hα	6563	12	600	1.54	85 Dec. 13
Hα	6563	78	600	1.54	86 Jun. 23
Hα	6563	78	300	1.54	86 Jun. 23
Cont.	6646	78	300	1.54	86 Jun. 23
[S II]	6740	85	300	1.54	86 Jun. 23
Gunn g	~5000	~1200	300	1.54	86 Jun. 23
Gunn g	~5000	~1200	60	1.54	86 Jun. 23
Gunn r	~6500	~ 900	30	1.54	86 Jun. 23
Gunn i	~8150	~1900	30	1.54	86 Jun. 23
Gunn z	>8500	~2500	60	1.54	86 Jun. 23
Gunn z	>8500	~2500	120	1.54	86 Jun. 23

integrated all-over N 81 (~20 pixels) and one-pixel spectra showing the variation of emission lines across N 81. We found for four spectra of the first kind $r = 2.92 \pm 0.04$, while the value derived for 12 individual spectra was $r = 2.96 \pm 0.07$. The value obtained for both kinds of spectra was 2.95 ± 0.07.

The nebular line intensities were corrected for interstellar extinction using a reddening function $f(\lambda)$ for the LMC parametrized by Howarth (1983). In the spectral range studied here the reddening law is the same in the LMC and SMC. The intensities of the main nebular lines are presented in Table 2, where $F(\lambda)$ and $I(\lambda)$ give observed and de-reddened line intensities. The uncartainties are indicated by the capital letters: A < 10%, B = 10–20%, C = 20–30%, D = 30–40%, and E > 40%. The lines marked with "ab" appear in absorption.

2.1.3. CAT/CES

The 1.47 m Coudé Auxiliary Telescope (CAT) and the Coudé Echelle Spectrograph (CES) were used on January 16, 1987 at La Silla to carry out high resolution spectroscopy of N 81 (resolving power 80000). The detector was a high resolution RCA CCD chip of type SID 503 (1024 × 640 pixels, each pixel 15 μm × 15 μm, corresponding to about 1″ in the dispersion direction). The spectral range covered about 40 Å centered at Hβ. The slit width was 1″.5 and the exposure time 30 min.

2.2. CCD imagery

Narrow and wide band pictures of N 81 were obtained using a CCD camera attached to the 3.60 m and 1.54 m telescopes at La Silla.

2.2.1. 3.60 m

The ESO Faint Object Spectrograph and Camera (EFOSC) at the 3.60 m telescope was used on November 19, 1985 to obtain direct images of N 81 (for a description of performances of this instrument see the EFOSC operating manual or Buzzoni et al., 1984). The detector was a high resolution CCD chip with characteristics as explained in Sect. 2.1.3.

2.2.2. 1.54 m

The CCD used at the Danish telescope was a RCA thinned backside illuminated SID 53612, 512 × 320 pixels, each pixel 30 μm × 30 μm, corresponding to 0″.47 × 0″.47 on the sky.

The CCD images were reduced (debiasing, flat-fielding, cleaning, etc.) using the IHAP/HP and MIDAS/VAX image processing systems. Table 3 summarizes the log of the CCD frames.

2.3. Photometry

2.3.1. *UBVRI*

The single channel photometer was used at the Cassegrain focus of the ESO 1 m telescope on 1985 July 17, and 1986 September 20 to obtain *UBVRI* photometry of N 81. The photomultiplier was a Quantacon tube of type 31034 A.

Each night at least 10 standard stars, taken from Graham's (1982) catalog, were observed at various airmasses. The data were reduced using the ESO reduction program SNOPY. The uncertainties on magnitudes and colors were less than ±0.03. The results are: $V = 11.49$, $B-V = 0.73$, $U-B = -0.84$, $V-R = -0.58$, $V-I = -0.97$.

Table 4. Star positions (1950.0) for the field of N 81

Iden.	α (h m s)	δ (° ′ ″)
N 81	1 7 45.61	−73 27 38.88
1	1 7 47.98	−73 27 27.87
2	1 7 49.28	−73 27 20.94
3	1 7 53.89	−73 27 19.18
4	1 7 55.62	−73 27 12.50
5	1 7 57.32	−73 27 07.65
6	1 7 50.89	−73 26 44.70
7	1 7 39.50	−73 27 24.13
8	1 7 39.83	−73 27 13.79
9	1 7 35.74	−73 27 31.39
10	1 7 32.22	−73 27 20.14
11	1 7 28.42	−73 27 15.91
12	1 7 35.47	−73 27 50.45
13	1 7 30.73	−73 28 06.91
14	1 7 43.27	−73 28 10.15
15	1 7 44.52	−73 28 09.91
16	1 7 46.76	−73 28 01.27
17	1 7 51.48	−73 27 52.21
18	1 7 41.68	−73 28 27.96
19	1 7 36.95	−73 28 39.30
20	1 7 36.48	−73 28 31.28
21	1 7 34.66	−73 28 33.08
22	1 7 32.00	−73 28 33.01
23	1 7 52.41	−73 26 44.72
24	1 7 52.70	−73 26 57.67
25	1 7 41.09	−73 27 12.34
26	1 7 44.84	−73 27 05.61
27	1 7 46.85	−73 27 53.10
28	1 7 48.60	−73 27 49.94
29	1 7 38.71	−73 28 34.26

2.3.2. *JHK* photometry

Near infrared broad-band photometry was performed on two opportunities (September 1985 and August 1986) using the ESO 1 m telescope equipped with its standard photometer and an InSb detector. Beam switching was operated in the East-West direction with an amplitude of 30″. In a diaphragm of 15″, we obtained $J = 12.08$, $H = 12.13$ and $K = 11.60$ accurate to ± 0.10 mag. Measurements were acquired also with diaphragms of 22″ and 30″, but no extension was detected at a significant level. However, comparison of our results with those of Koornneef and Israel (1985) shows that the object, in a 15″ diaphragm, is ~0.15 mag brighter than in a 10″ diaphragm, and ~0.5 mag than in a 7.″5 one. Therefore, the continuum emission in the 1–2.5 μm range appears to be extended up to 7 to 8″ from the peak. There is no indication of a color effect from diaphragm to diaphragm.

2.4. Astrometric measurements

Although the Magellanic Clouds are the nearest external galaxies, we are suffering from lack of detailed information on them in many respects. For example, stellar positions are in general poorly known. In order to increase our information on N 81 in particular and on this region of the SMC in general, we give accurate positions for objects lying in this direction.

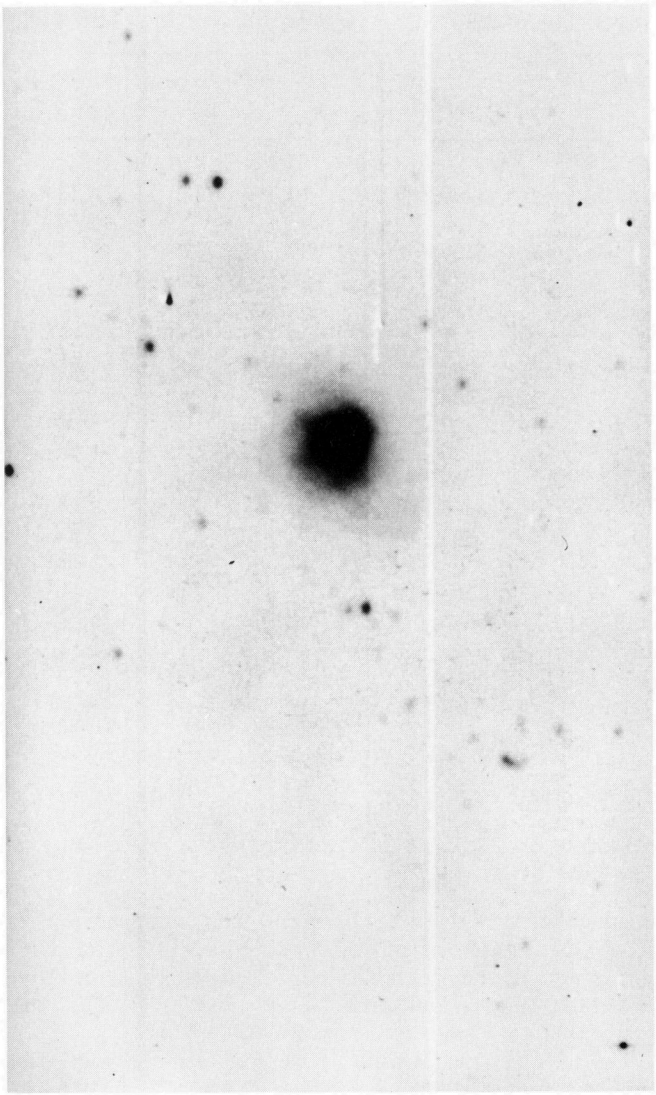

Fig. 2a. Hα

Fig. 2a–h. The CCD frames obtained towards N 81. **a** Hα; **b** Hβ, logarithmic grey scale; **c** [O III]; **d** He II; **e** [O II]; **f** No. 1402; **g** *V*; **h** Gunn *r*. The field corresponds to 143″ × 248″, except for the Hβ which represents 59″ × 61″ on the sky and the EFOSC frame *V* which corresponds to 218″ × 354″. The images are not corrected for stellar continuum. North is at the top, east to the left

The position of N 81 along with those of 29 stars lying in the same field were measured on the ESO B plate obtained at the ESO Schmidt telescope (see West and Schuster, 1982). The measuring machine was the ESO Garching Optronics which allows determination of accurate positions. The calibration was carried out using 15 Perth standard stars lying in the direction of N 81 on the field number 29. The rms deviations in α and δ were 0.″32 and 0.″42, respectively. Table 4 gives the measured positions for the stars labelled on the *V* frame (Fig. 2g).

3. Morphology and brightness

The nebula N 81 is a compact star-looking object lying at more than 1° SE of the SMC "bar". Two unknown star clusters are visible at about 35″ and 75″ south of N 81, corresponding to about

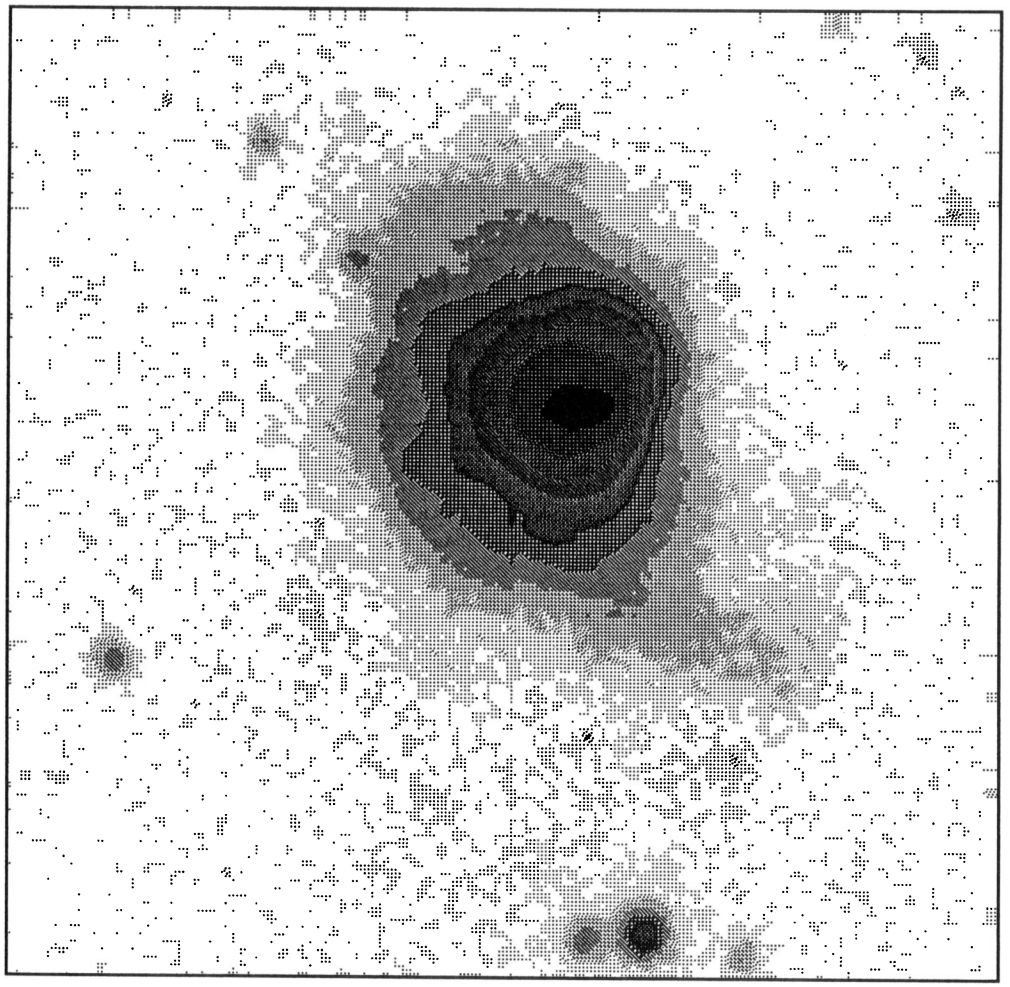

Fig. 2b. Hβ

11 and 22 pc respectively. On long-exposure broad-band pictures these clusters merge forming a tail structure for N 81. However, they are probably not linked to N 81.

The CCD Hα, Hβ and [O III] frames of N 81 show a very bright compact core surrounded by a diffuse envelope (Fig. 2a–c). The core appears clearly on the high excitation He II 4686 frame (Fig. 2d) as well as on the continuum 4794 (Fig. 2f). The envelope seems more or less circular except towards SW where it turns into a slight curling structure. The envelope appears more diffuse on the [O II] 3727 + 3729 frame (Fig. 2e) showing a spectacular structure.

Cross-cuts were obtained along several orientations in various CCD images. Figure 3 shows an important feature. The core of N 81 comprises at least three components. Moreover, we see sharp ridges towards north and west borders and envelope extension in other directions.

The profiles passing through intensity peaks were approximated by Gaussians. Table 5 gives the FWHM's obtained along EW and NS directions. N 81 has the same FWHM in the Balmer hydrogen lines Hα and Hβ as in the high-excitation line [O III] 5007, while it is less extended, by a factor of about 3.5, in the He II line and the continuum at 4794 Å (filter 1402).

N 81 is, almost in all lines, more extended in EW direction than in NS. We adopt a Gaussian radius in Hβ, $\theta_G = (\theta_\alpha \times \theta_\delta)^{1/2} = (13.4 \times 13.6)^{1/2} = 6''.3$ for N 81.

The total Hβ flux of N 81 was derived using the following procedure. First we calculated the relative Hβ flux in an imaginary 4″ slit passing through the Hβ CCD frame. This value was then compared with the absolute Hβ flux obtained from the CCD spectra. In both cases a mean flux obtained for the NS and EW orientations of slit was used. The total Hβ flux thus obtained was $F(\mathrm{H}\beta) = (1.45 \pm 0.20)\ 10^{-11}\ \mathrm{erg\,cm^{-2}\,s^{-1}}$. This value is by a factor 1.7 larger than that observed by DH corresponding to a $10'' \times 78''$ aperture not covering the whole nebula. From the reddening corrected Hβ flux (Table 2), we evaluate the luminosity of N 81 at Hβ to be about $9.3\ 10^{36}\ \mathrm{erg\,s^{-1}}$, or $2400\ L_\odot$. This luminosity corresponds to a flux of $2.28\ 10^{48}$ Hβ photons $\mathrm{s^{-1}}$.

4. Temperature and density

4.1. *Temperature*

The electron temperature, T_e, was derived from the intensity ratio, R, of the nebular $(^1D\text{–}^3P)$ 4959 + 5007 Å and the auroral $(^1S\text{–}^1D)$ 4363 Å transition of [O III]. A three level atom was used to calculate the corresponding emissivities. The atomic parameters where those compiled by Mendoza (1983).

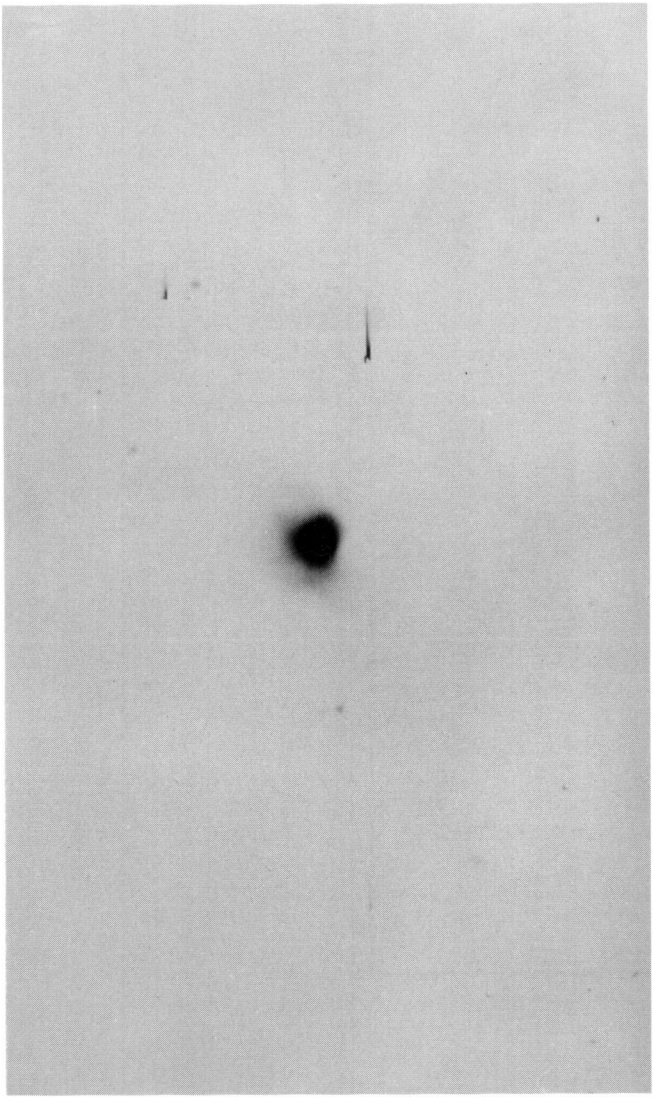

Fig. 2c. [O III]

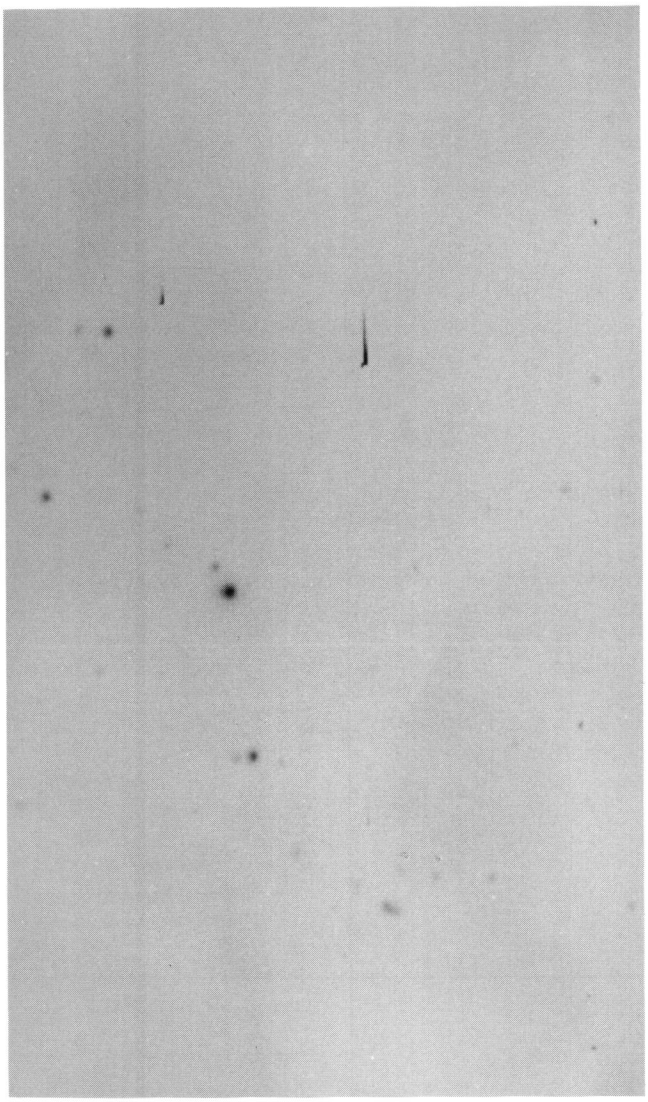

Fig. 2d. He II

It is very important for the abundance determinations to have very accurate values of T_e. The accuracy on the T_e determination is mainly based on the precision to which the [O III] 4363 Å line is measured. This line being well separated from the Balmer Hγ line in the 59 Å mm^{-1} CCD spectra, has a S/N ratio of about 100. Assuming 5% errors on the nebular and auroral transitions of [O III], we derive, from $R = 80.9 \pm 0.8$, $T_e = 14100 \pm 360$. Note that DH find $T_e = 12150 \pm 500$ from $R = 109$.

The [O III] temperature derived here for N 81 is about 15% higher than that obtained by DH. This mainly results from the lower R ratio obtained in the present work, but also partly from the use of new atomic parameters (Mendoza, 1983).

It was impossible to derive the temperature from the ratio of the [N II] lines 5755/(6584+48) with a good accuracy, because of poor S/N ratio on the [N II] 5755 line.

4.2. Density

The electron density was obtained using two methods. In the first one the ratio of the (^2S–^2D) doublet of [S II] 6717, 31 was used. We derive $N_e = 420\,\mathrm{cm}^{-3}$ corresponding to the total [S II] line intensities integrated in a 4″ slit. In the second method the total Hβ flux (Sect. 3) was used to derive a rms electron density. The result was $330\,\mathrm{cm}^{-3}$, indicating a filling factor of 0.89. The distance of the SMC was taken to be 66 kpc (Azzopardi, 1981).

5. Chemical abundances

The line intensities given in Table 2 were used to derive the abundances of several elements in N 81. The method has been explained elsewhere (Heydari-Malayeri and Testor, 1986). The wide spectral range covered in this work made available various spectral lines of the same element at different excitation levels. This is essential for accurate determination of total abundances. Tables 6 and 7 give the ionic and elemental abundances with respect to hydrogen. Some comments are in order as to the abundance results.

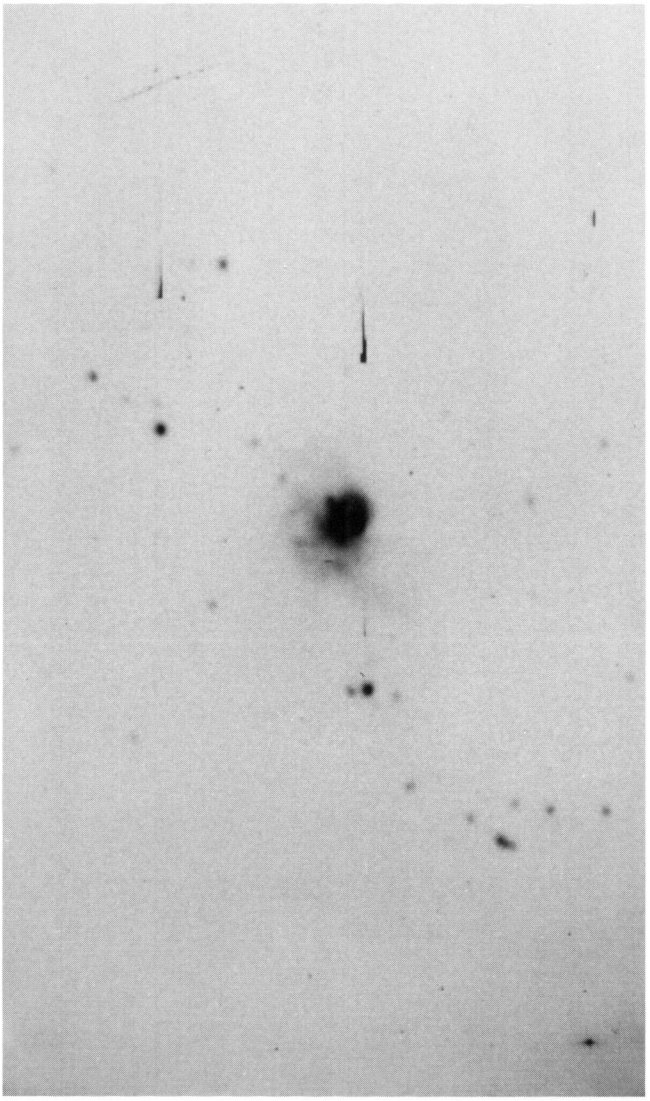

Fig. 2e. [O II]

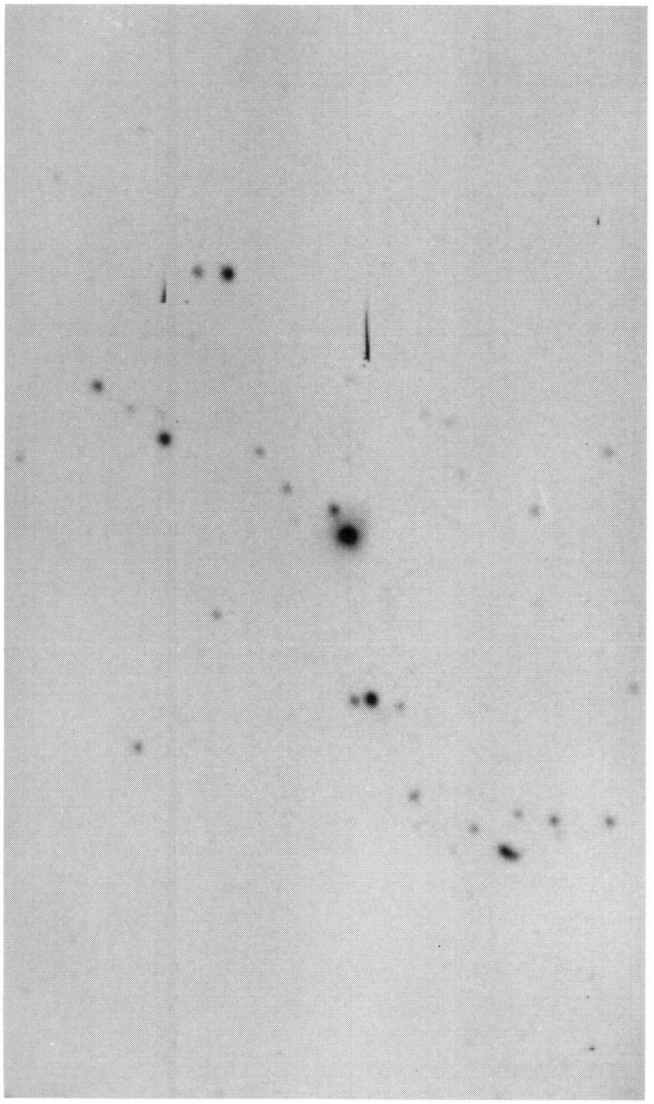

Fig. 2f. No. 1402

5.1. *Helium*

The ionic abundances were derived separately from three recombination lines at 4471, 5876, and 6678 Å. The adopted ionic abundance represents an average value in which He^+ (5876) has a weight of 2. The chosen weights are based on the relative intensity of the lines. The He^+ abundances are rather insensitive to the temperatures used in the calculations. The errors in He^+ abundances are probably less than 15%.

In order to derive the total He abundance we should correct the above value for neutral He in the object. Such corrections are important for dense nebulae with exciting stars having $T_{\rm eff} < 37000$ K (Osterbrock, 1974). In the case of N 81 the correction for neutral helium should be quite small (see, e.g., DH). Moreover, our deep CCD spectra do not show the presence of nebular He II lines. Therefore, we conclude that all the He in N 81 is in the form of He^+. Consequently, we assume an ionization correction factor of unity for He.

5.2. *Oxygen*

The abundance of the oxygen ion O^+ was calculated from two different pairs of transitions [O II] 3727,29 and 7319,30 Å. N 81 is one of the rare SMC H II regions for which O^+ abundance has been derived from the [O II] 7319,30 doublet. There is $<10\%$ difference between the two determinations. This seems quite good, given the accuracy of the line intensities. We adopt a mean value of $1.42\ 10^{-5}$ for the abundance of O^+ ions (Table 6). Our result is about 70% lower than that found by DH. This is mainly due to the fact that O^+ abundances are particularly sensitive to the electron temperature used. The abundance of O^{++} is also sensitive to the T_e, but to a lesser extent. We find about 45% less of O^{2+} ions in N 81 with respect to DH.

In determining the elemental abundance of O it was supposed that this element is principally in the form of O^+ and O^{2+}. Therefore, no ionization correction was used. Our result (Table 7) is about 50% smaller than that obtained by DH for N 81 and 30%

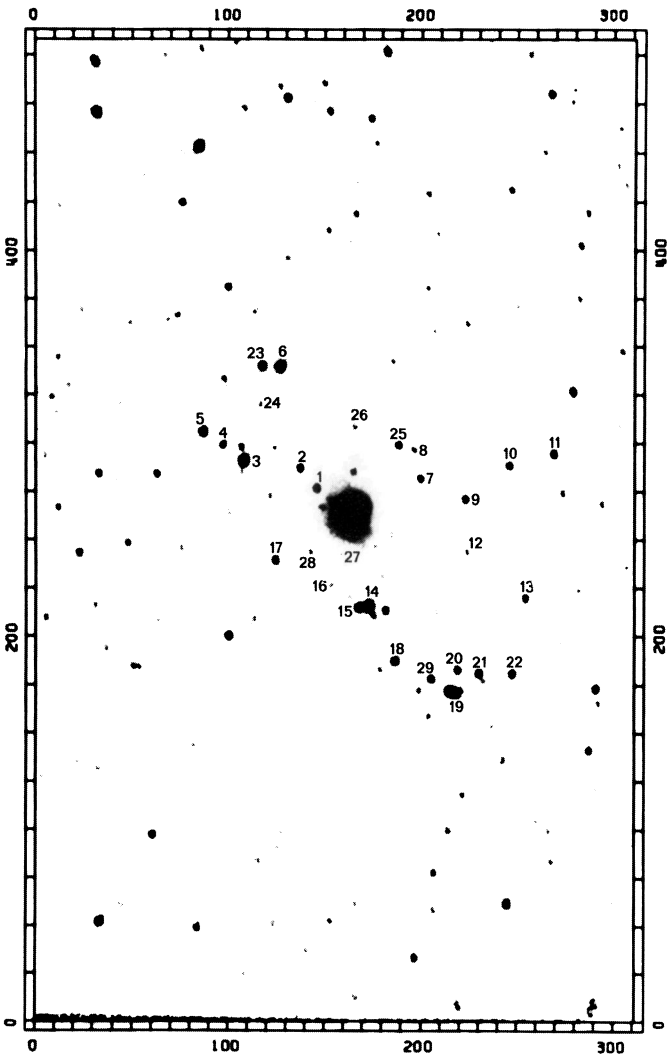

Fig. 2g. *V*

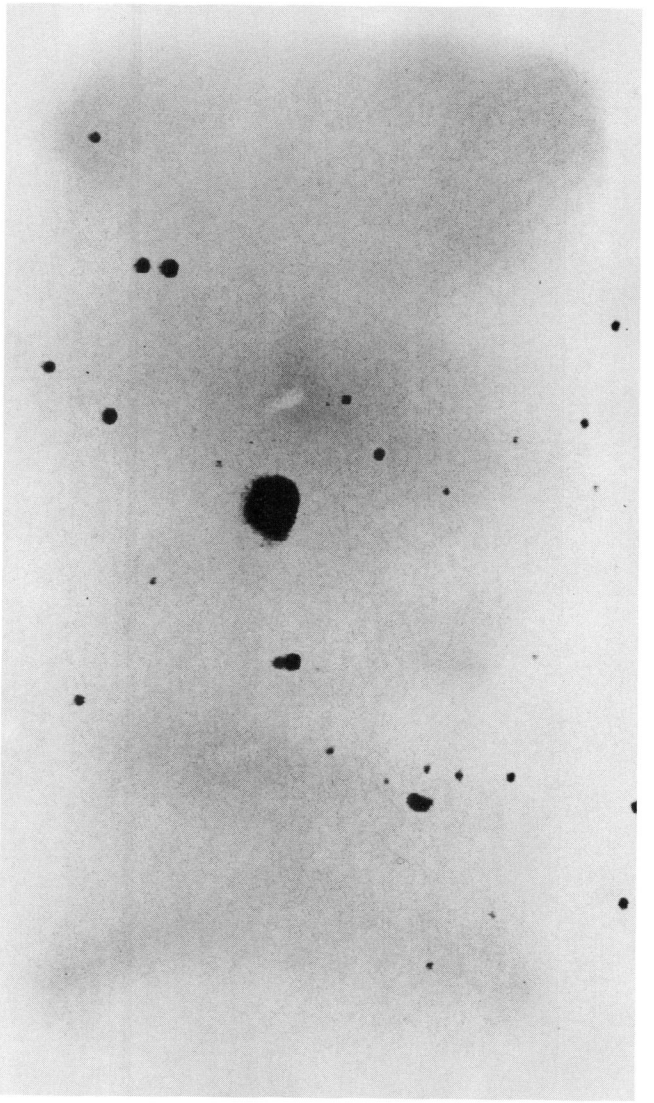

Fig. 2h. Gunn r

below the average O abundance attributed to the SMC (Dufour, 1984). The derived O abundance in the present work is probably correct within 50%.

5.3. *Nitrogen*

The N^+ abundance (Table 6) does not depend strongly on the electron temperature T_e. The largest errors come from the uncertainty on the 6548,83 lines intensities. Our results is accurate within 30%.

The ionization correction factor for N, deduced from the Peimbert and Torres-Peimbert (1977) approach, is large (5.8). However, our result agrees within 30% with the mean SMC value (itself obtained with about 70% accuracy).

5.4. *Neon*

The abundance of Ne^{2+} is very sensitive to T_e, but the ionization correction factor is smalll and the 3869 line was measured more accurately than 10%. The total abundance agrees with the SMC mean value within about 10%.

5.5. *Sulphur*

The abundance of S^{++} derived from the line 6312 Å is very sensitive to the temperature used. Moreover, there could be substantial errors in the measurement of 6312 due to the presence of [O I] 6300 Å. Therefore it is better to derive the S^{2+} abundance from the measurement of the strong [S III] lines 9069–9532 Å which allow derivation of reliable sulphur abundance in objects of moderate excitation. In order to correct for the atmospheric absorption affecting the [S III] line at 9532 Å, the theoretical value of the intensity ratio [S III] 9532/9069 was used. The total [S III] intensity was taken equal to 3.44 times that of the 9069 line which is less absorbed compared with the 9532 line. Our S^+ results is about a factor 2.5 smaller than that obtained by DH, who have not observed S^{++} lines.

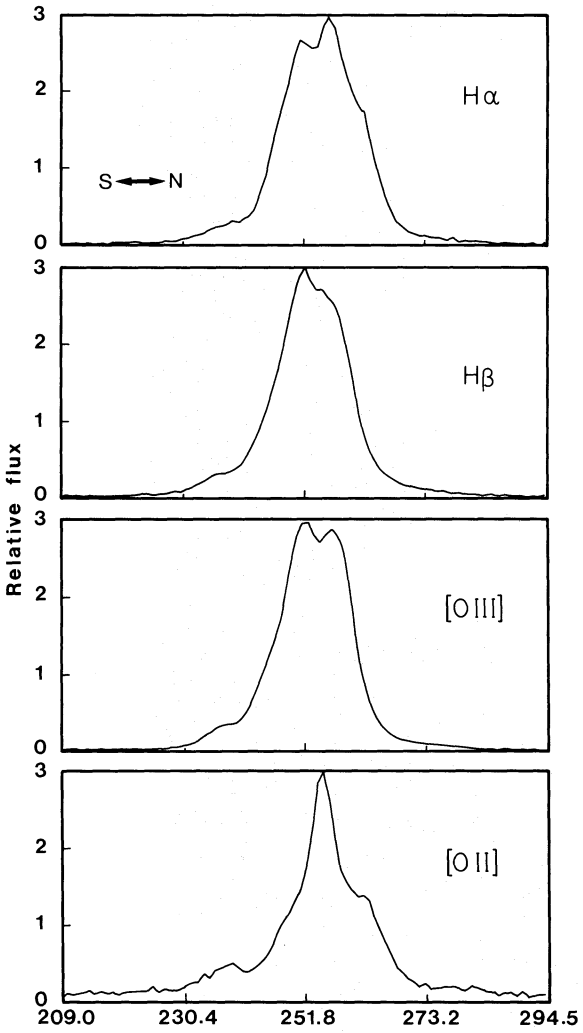

Fig. 3. Cross-cuts obtained through the CCD frames along the NS direction. Abscissa represents pixel positions

Table 5. N 81 profiles in various lines

Line	EW	NS	NESW
Hα	14.0	11.9	12.7
Hβ	13.4	13.6	13.4
[O III]	13.8	13.5	13.5
He II	4.0	3.7	4.0
No. 1402	4.8	4.4	
Cont.	5.2	4.2	
V 2 min	9.9	7.9	
B 2 min	7.5	6.1	
V 1 s	5.2	4.8	
B 3 s	4.7	3.9	
U 20 s	3.9	4.0	

Table 6. Ionic abundances $N(X^+)/N(H^+)$ for N 81

Ion	This work	DH
He^+ (4471)	$9.55\ 10^{-2}$	
He^+ (5876)	$8.56\ 10^{-2}$	
He^+ (6678)	$8.66\ 10^{-2}$	
He^+ (adopted)	$8.83\ 10^{-2}$	0.085
O^+ (3727)	$1.37\ 10^{-5}$	$2.47\ 10^{-5}$
O^+ (7327)	$1.47\ 10^{-5}$	
O^+ (adopted)	$1.42\ 10^{-5}$	
O^{2+} (4959+5007)	$6.49\ 10^{-5}$	$9.46\ 10^{-5}$
N^+	$3.75\ 10^{-7}$	$6.46\ 10^{-7}$
Ne^{2+}	$1.23\ 10^{-5}$	$1.85\ 10^{-5}$
S^+ (6717+31)	$1.03\ 10^{-7}$	$3.76\ 10^{-7}$
S^{2+} (9532)	$5.31\ 10^{-7}$	–
Ar	$3.79\ 10^{-7}$	–

Table 7. Elemental abundances $N(X)/N(H)$ for N 81

Element	This work	DH	⟨SMC⟩
He	0.088	0.085	0.080±0.003
O	$7.91\ 10^{-5}$	$1.19\ 10^{-4}$	$1.05\ 10^{-4}$
N	$2.16\ 10^{-6}$	$3.12\ 10^{-6}$	$2.88\ 10^{-6}$
Ne	$1.49\ 10^{-5}$	$2.34\ 10^{-5}$	$1.66\ 10^{-5}$
S(A)	$6.34\ 10^{-7}$	–	–
S(B)	$1.12\ 10^{-6}$	$1.82\ 10^{-6}$	$3.09\ 10^{-6}$
Ar	$7.58\ 10^{-7}$	–	$6.03\ 10^{-7}$

Two values are given for the total sulphur abundance in Table 7. S(A) was obtained assuming that the only S ions present are S^+ and S^{2+}. The S(B) value is the sulphur abundance corrected for the unobserved ions (Dennefeld and Stasińska, 1983). This value is more than a factor 2 smaller than that given by Dufour (1984) for the mean SMC S abundance.

5.6. Argon

The [Ar III] line at 7136 was measured with an accuracy of 15%. The ionization correction factor used was 2. The Ar abundance is weakly dependent on the T_e used. Our result is about 25% larger than the mean Ar abundance for the SMC.

Generally speaking, our abundance values are smaller than those derived by DH and, to a lesser degree, than the mean SMC abundances. This is mainly due to the higher T_e value, different atomic parameters (Mendoza, 1983) and different ionization correction factors used. We ran our abundance code using the line intensities listed in Table 2, except for the oxygen lines for which we used the intensities reported by DH. The resultant temperature agrees within ~5% with DH's value. That is the same for the O and Ne elemental abundances which are temperature sensitive. For nitrogen abundance the result is ~15% smaller than DH's, probably due to their higher [N II] 6583,48 line intensity (~45%). In the case of S we find a total abundance ~30% smaller than the value given by DH. This is probably due to different atomic parameters used, to the fact that DH did not observe the lines necessary for computing S^{++} abundances and to the ionization correction factor. Note also that the S abundance given by DH is ~70% smaller than the mean SMC estimate.

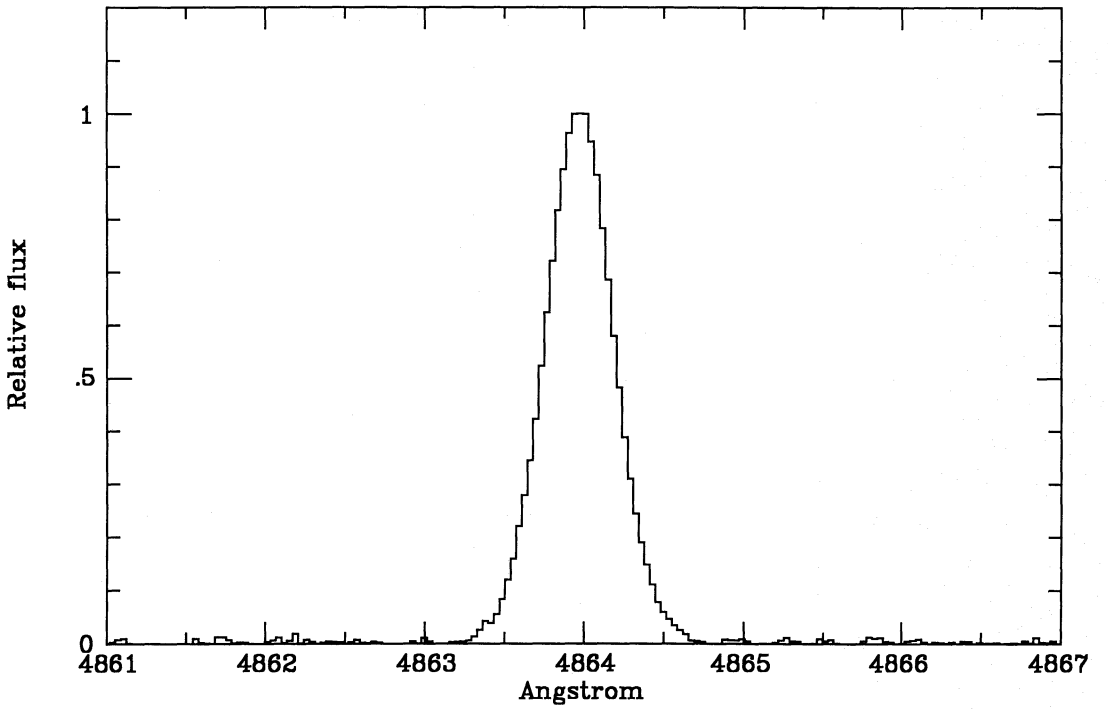

Fig. 4. The Hβ profile of N81 obtained using the CES at the ESO CAT telescope

6. Velocity

The Hβ profile obtained using the CAT/CES system is displayed in Fig. 4. From the measured wavelength shift, $\Delta\lambda = 2.627$ Å, a heliocentric radial velocity of $+158.8\,\mathrm{km\,s^{-1}}$ was derived for N 81, corresponding to a velocity of $144.8\,\mathrm{km\,s^{-1}}$ with respect to the Local Standard of Rest. The estimated uncertainties in the determination of the radial velocity is about $1\,\mathrm{km\,s^{-1}}$. Our radial velocity referred to the Sun is in good agreement with Smith and Weedman's (1973) value, $+161.0 \pm 2.5\,\mathrm{km\,s^{-1}}$ based on [O III] 5007 profiles. Feast (1970) derived a radial velocity of $+157\,\mathrm{km\,s^{-1}}$ for N 81 from Hα measurements.

We use McGee and Newton's (1981, 1982) H I survey of the SMC to compare the radial H II and H I velocities obtained towards N 81. These authors found that the H I gas in the SMC exists in four distinct components at velocities about +115, +134, +167, and $+192\,\mathrm{km\,s^{-1}}$ respectively.

We see that for the position corresponding to the H II region N 81 the H I has a component at $162.8\,\mathrm{km\,s^{-1}}$. The line width at hlaf maximum is $23.6\,\mathrm{km\,s^{-1}}$ and the column density of the neutral hydrogen $N_{\mathrm{H}} = 2.9\ 10^{21}$ atoms cm^{-2}. Around this point, for the same right ascension, the velocity varies from 161.7 to $165.5\,\mathrm{km\,s^{-1}}$ in a region more than two times the beam size of the telescope (15′). For the same declination, the H I velocity increases systematically eastward from 153.3 to $171\,\mathrm{km\,s^{-1}}$ in a region three times the beam. We conclude that N 81 is probably associated with the H I component having the mean radial velocity of $167.1 \pm 8.0\,\mathrm{km\,s^{-1}}$. Note that the velocity peak at $171\,\mathrm{km\,s^{-1}}$ corresponds to the position of the H II complex N 83/N 84 lying at about 30′ east of N 81. There, the column density of H I rises to 3.5 10^{21} atoms cm^{-2}.

The Hβ profile (Fig. 4) can very nicely be fitted by a Gaussian of FWHM = 0.494 Å, corresponding to an internal velocity of $30.5\,\mathrm{km\,s^{-1}}$. The instrumental broadening was measured to be 0.061 Å, corresponding to a velocity of $3.8\,\mathrm{km\,s^{-1}}$. The thermal broadening for an H II region with electron temperature 14100 K (Sect. 4.1) is expected to reach 0.411 Å, corresponding to a thermal velocity of $25.4\,\mathrm{km\,s^{-1}}$. Consequently, if we assume a Gaussian profile for the components, we derive an excess velocity dispersion of $16.5\,\mathrm{km\,s^{-1}}$ in N 81. In the following we consider the meaning of this excess dispersion.

The excess may probably be due to the sum of two components, one turbulent and the other the expansion velocity of the H II region. Recently, several investigations have addressed the turbulence issue in a number of H II regions. They have found that there is a dependence of the random velocity upon scale, arguing for the presence of turbulence (O'Dell and Castañeda, 1987; Roy et al., 1986). From the set of data given by O'Dell and Castañeda (1987) for the galactic H II regions NGC 1499, 6514, 6523 A, 7000, S 252, and NGC 6523 B two distinct power law relationships can be derived between the most probable one-dimensional turbulent velocity, W, and the diameter of the observed area, d. The data for the first five cited regions (25 points) are well-aligned. So, we can derive the following relation for them:

$$W(\mathrm{km\,s^{-1}}) = 1.06\ d^{0.40}\,(\mathrm{pc})\,. \tag{1}$$

By contrast, the relation for NGC 6523 B (8 points) is quite flat:

$$W = 2.66\ d^{0.07}\,. \tag{2}$$

Applying these two relations to N 81 ($d = 4$ pc), we find the most probable one-dimensional turbulent velocities of 1.8 and $2.9\,\mathrm{km\,s^{-1}}$, leading to three-dimensional turbulent velocities of 2.2 and $3.5\,\mathrm{km\,s^{-1}}$ respectively. If we assume a Gaussian profile for the expansion motion of N 81, we find expansion velocities of 16.4 and $16.1\,\mathrm{km\,s^{-1}}$ respectively. As the expansion goes on in directions towards and away from us, these values should be divided by two. Consequently, we get an expansion velocity of about $8\,\mathrm{km\,s^{-1}}$, which is not supersonic.

Koornneef and Israel (1985) detected near infrared molecular hydrogen emission towards N 81. There are two mechanisms proposed to explain the H_2 emission: 1) Ultraviolet pumping and associative detachment; 2) Collisional excitation in a shocked region. The present result suggests that the second mechanism may, at least partly, be responsible for the H_2 emission. Thus, we observationally confirm the proposition by Koornneef and Israel (1985) that the H_2 molecular emission may be produced by the action of a mild shock moving through the ambient cloud of N 81.

7. Excitation and stellar content

We use the ionization and recombination equilibrium relations to get the following formula between the Lyman continuum flux, N_L, and the number of Hβ photons emitted by the nebula, N_β:

$$N_L = 6.08\, T_e^{0.04}\, N_\beta, \quad (3)$$

where T_e is the electron temperature in Kelvins. Using $N_\beta = 2.28\ 10^{48}$ ph s^{-1} (Sect. 3) and $T_e = 14100$ K (Sect. 4.1), we derive $N_L = 2.03\ 10^{49}$ ph s^{-1}.

This value is certainly a lower limit and should be corrected for possible photon losses. A fraction of the Lyman continuum photons may escape from the nebula in directions where it may be density-bounded. Therefore, these photons do not have Hβ representatives. Mezger (1978) estimated the fraction of photons which can escape the density-bounded (extended low-density) H II regions to amount to as high as 70%. Likewise, the Hβ flux integrated over N 81 should be corrected for the orientation of the object. We are probably looking at N 81 with an angle. Therefore, a fraction of the nebula may be hidden by its associated molecular cloud, as it is the case for most young galactic H II regions. In contrast, the loss due to absorption by dust is negligible for N 81 (Sect. 8). Consequently, we assume, somewhat arbitrarily, that the total loss may amount to some 30%. This gives a new value for the Lyman continuum flux, $N_L = 2.9\ 10^{49}$ ph s^{-1}.

The [O III] (4959+5007)/Hβ intensity ratio for N 81 amounts to 6.94 (Table 2). It is clear from past research (e.g., Stasińska, 1980; Mathis, 1982) that this ratio is not a good indicator of excitation, because it depends on a combination of ionizing flux, filling factor, gas density and metal abundance in the H II region. Several authors have used an "ionization parameter" defined as $Q = (N_H f^2 N_L)^{1/3}$. For N 81 we derive $Q = 2.0\ 10^{17}$ cm^{-1} s$^{-1/3}$ indicating a high excitation H II region. The average ionization parameter derived by McCall (1982) for 99 H II regions in 20 spiral and irregular galaxies is $3.8\ 10^{15}$ cm^{-1} s$^{-1/3}$. For comparison purposes we derive the Q-values for the SMC H II blob N 88 A and the LMC blob N 160 A1. From the Hβ flux given by Testor and Pakull (1985) we derive $N_L = 2.72\ 10^{49}$ ph s^{-1} for N 88 A, leading to a Q-value more than 80% higher than that for N 81. For N 160 A 1 (Heydari-Malayeri and Testor, 1986) we find a Q-value about 50% higher.

7.1. Exciting star(s)

We use the evolutionary tracks in the (log L, log T_{eff}) plane from Chiosi et al. (1978) for the ZAMS stars of initial masses 100, 80, 60, 40, and 20 $M_\odot$ (high mass loss factor, $\alpha = 0.90$) together with the stellar atmosphere models of Kurucz (1979) for solar metal abundances. The derived Lyman continuum flux implies that N 81 may be excited by one star of about 60 $M_\odot$ with $T_{eff} = 47500$ K and continuum emission at Hβ of $2.67\ 10^{33}$ erg s^{-1} Å^{-1}. The spectral type of such a star should be earlier than O 5 V (Panagia, 1973). Alternatively, it is possible that N 81 be excited by two 40 $M_\odot$ stars with $T_{eff} = 44000$ K, corresponding to a spectral type earlier than O 6.

Direct observational evidence supports the idea that the exciting source of N 81 is a hot main sequence star. Our spectra clearly show He II absorption lines at 4200, 4541, 4686, and 5412 Å (Table 2). The He II line at 4686 Å is particularly prominent, with an equivalent width of 0.64 Å. The profiles of the He II absorption lines are wider than those of emission lines. For example, the FWHM of He II 4686 is 6.0 Å, while the mean FWHM of the emission lines is 3.1 Å. This is probably due to substantial motions in the outer atmosphere of the star.

Unfortunately, we cannot derive an accurate spectral type for this star, due to contamination of He I absorption lines by the corresponding nebular lines. While the stellar Balmer lines Hε, Hδ and Hγ show up as weak absorptions in the wings of the corresponding emission lines, there is no hint for the presence of He I absorption at 4471 Å. The nebular intensity ratio Hδ/He I 4471 Å is about 6 (Table 2). From an inspection of published spectra for O 5–O 6 stars, we deduce that this ratio for absorption line should be of the same order, if not smaller. Therefore, the He I 4471 line also should appear in the wing of the nebular line. We conclude the absorption line at 4471 Å is probably very weak, in agreement with the presence of an early O type star.

7.2. Excitation parameter and mass

We deduce the excitation parameter to be:

$$u = 2.45\ 10^{-16}\, (N_L\, T_e^{0.83})^{1/3}, \quad (4)$$

where N_L is the Lyman continuum flux and T_e the electron temperature in K. We derive $u = 106$ pc cm^{-2}, in agreement with a spectral type O 5 V (Panagia, 1973).

The mass of ionized gas, in solar units, can be derived from the following formula:

$$M = 2.70\ 10^8\, (1+4y)\, T_e^{0.87}\, D^2\, n_e^{-1}\, I_\beta, \quad (5)$$

where y is the number abundance of helium (Sect. 5), D the distance in kpc, n_e the rms electron density and I_β the Hβ intensity in erg cm^{-2} s^{-1}. The derived mass is about 350 $M_\odot$.

7.3. Equivalent width of Hβ

The continuum flux at Hβ is measured to be $2.9\ 10^{-14}$ erg cm^{-2} s^{-1} Å^{-1}. This gives a total emitted continuum at Hβ of $1.52\ 10^{34}$ erg s^{-1} Å^{-1}, for a distance of 66 kpc. The Hβ equivalent width (EW), not corrected for the reddening (Sect. 8), is 200 Å.

We derive the EW of the Hβ emission to be:

$$W_\beta = 5.59\ 10^{-57}\, T_e^{-0.04}\, D^{-2}\, f_\beta^{*-1}\, N_L, \quad (6)$$

where T_e is the electron temperature in K (Sect. 4.1); D the distance in kpc; f_β^* the continuum at Hβ in erg s^{-1} cm^{-2} Å^{-1} and N_L the Lyman photon flux. Using this relation, we would predict an Hβ EW of 613 Å.

So, there is a significant discrepancy between the measured and expected EWs. Two explanations can be proposed. The H II region may be density-bounded. This means that the emission surface brightness is small with respect to the continuum surface brightness. In other words, the volume of gas available for

ionization is smaller than the volume the exciting star(s) are capable of ionizing. However, the intensity of the [O III] 5007 Å line does not appear to be abnormally high relative to that of [O II] 3727, as should be the case for a density-bounded H II region. But N 81 might be density-bounded in directions where we lack spectra.

Alternatively, the continuum emission may be higher than expected for an ionizing star of a given Lyman flux. This excess may be due to the presence a cluster of B stars which do not play a role in ionization but predominantly contribute to the continuum emission. This result is supported by Koornneef and Israel (1985) who observed a relatively strong near infrared continuum, especially at 3.76 μm. They argue that since it is unlikely that there is dust hot enough to emit at this wavelength, the excess continuum should be due to lower mass stars.

If we adopt the hypothesis that the nebula is ionized by a single 60 $M_\odot$ star, the excess continuum is 1.3 10^{34} erg s^{-1} Å^{-1}. It could be provided by about 40 B0V stars, with mass 15 $M_\odot$ and $T_{\rm eff} = 32000$ K. An even larger number of A stars would be necessary to account for the continuum. The assumption of two stars of 40 $M_\odot$ does not significantly decrease this number. This high number of stars in a volume of about 2 pc in radius does not seem realistic.

Let us now examine the contribution of atomic processes to the observed continuum. The main sources of nebular continuum are hydrogen and helium free-bound, free-free and two quantum emissions. Using the emission coefficients tabulated by Pottasch (1984), we derive the following relation for the nebular continuum flux relative to that of the Hβ emission line:

$$I_c/I_\beta(\text{Å}^{-1}) = 1.25\ 10^{-3}\ \lambda^{-0.11} + 1.49\ 10^{-4}\ \lambda^{-0.13} + 7.42\ 10^{8}\ \lambda^{-3,35}, \quad (7)$$

where λ is the wavelength in Å. This relation holds for 4000 Å $\leqq \lambda \leqq$ 7000 Å and $T_e = 14000$ K. The first and second right-hand terms represent the free-bound and free-free emissions of hydrogen and helium respectively. A helium ionic abundance of $N(He^+)/N(H^+) = 0.09$ was used (Sect. 5). The third term represents the two photon decay emission of hydrogen (for a parameter of 0.33). The collisional terms have been neglected, as the electron density is $< 5\ 10^4$ (Pottasch, 1984).

The above relation shows that at Hβ the atomic processes can contribute to about 55% of the total continuum. This result is confirmed by our analysis of the CCD continuum frame at 4794 Å obtained through the ESO filter No. 1402 (Table 3). The continuum profile of N 81 was deconvolved using a normalized point spread function represented by a typical field star on the frame. The N 81 profile was thus resolved into two Gaussians, one representing the exciting star and the other the nebula. It was found that at 4794 Å the nebular component contributes to more than 50% of the total continuum emission (nebular + stellar).

After correction for the nebular continuum, 13 B0 stars are necessary to provide the remaining continuum. A smaller number of B stars would be requested if the nebula is not completely ionization-bounded.

The distribution of stars among various mass intervals is represented by the initial mass function (IMF), of the form $\psi(M) \propto M^{-x}$. We use the IMF adopted by Lequeux et al. (1979) with $x = 2$. Hence, one 60 $M_\odot$ star is expected to be accompanied by 16 B0 stars of 15 $M_\odot$, while 2 stars of 40 $M_\odot$ require the presence of about 14 B0 stars. In both cases, these values agree with the number of B stars derived after the correction for the nebular continuum, stressing the necessity for this correction.

7.4. *Tentative magnitudes of the exciting star(s)*

We now try to estimate a visual magnitude for the exciting star(s) of N 81. The continuum flux at 5550 Å, when corrected for the nebular contribution, is 8.8 10^{-15} erg s^{-1} cm^{-2} Å^{-1}. Using Tüg et al.'s (1977) calibration for Vega, we derive $V \sim 14.0$. If we consider an uncertainty of 20% on the measured continuum, the uncertainty on the derived magnitude will be about 0.5. From the color $B-V = -0.30$ for early O stars (Conti et al., 1986), the B magnitude is estimated fo be ~13.7.

Adopting a distance modulus of $m-M = 19.1$ for the SMC (Azzopardi, 1981), we derive the absolute visual magnitude of the exciting star to be about −5.1. With a bolometric correction $BC = -4.0$, corresponding to O4–O5 stars (Humphreys and McElroy, 1984), we get a bolometric magnitude $M_b = -9.1$ for the star. The luminosity of this star should be about 3.5 10^5 $L_\odot$. Using the evolutionary tracks from models with mass loss calculated by Maeder (1981, 1983), we derive $T_{\rm eff}$ about 45000 K, in agreement with the result obtained from the Lyman continuum flux.

7.5. *Age estimate*

The Lyman continuum emission of the exciting star decreases with time. From Kurucz's (1979) stellar atmosphere models and the evolutionary tracks in the HR diagram from, e.g., Chiosi et al. (1978) for massive stars with mass loss, the Lyman continuum emission can be determined as a function of time. The time evolution strongly depends on the IMF, the upper mass limit and the metallicity.

The decrease of the Lyman continuum emission affects the continuum emission around Hβ. Therefore, the EW of Hβ can be used as an age indicator, if the H II region is ionization bounded. Several authors have developped models studying the time evolution of age indicator parameters. For example, Viallefond and Thuan (1983) consider two limiting models of star formation. The first one is the case of an infinitely short burst (ISB) and the second one a continuous star formation (CSF) with a constant star formation rate. In the ISB model, the EW of Hβ reaches zero after about 5 10^6 years due to the death of the massive stars. In the CSF model, the EW drops steeply during $\leqq 4\ 10^6$ years due to rapid decrease of the Lyman continuum luminosity but decreases slowly afterwards.

Here, to have a rough estimate for the age of N 81, we use the models calculated by Copetti et al. (1986) corresponding to an IMF with $x = 2$ and the chemical compositions of the SMC ($Z = 0.003$, $Y = 0.237$, $X = 0.76$). Two cases are considered: without mass loss and strong mass loss. From the measured EW for N 81, in the case of strong mass loss, we find the ages of 1.0 10^6 and 2.5 10^6 years corresponding to the upper mass limits 40 and 60 $M_\odot$ respectively. If there is no mass loss, which seems unlikely, the ages of 2.5 10^6 and 3.5 10^6 years will be derived respectively. This age estimate should be taken with precaution, because it is sensitive to errors in the stellar models, the IMF, the upper mass limit, the stellar content of the region and density bounding. These results may only confirm that N 81 is a young H II region.

8. Extinction

A color excess of $E(B-V) = 0.07$ can be derived for the ionized gas in N 81 using the Balmer decrement Hα/Hβ (Table 2). In deriving this value we have assumed a Galactic law for the

reddening in the SMC and $T_e = 14100$ K. Several authors have confirmed the Galactic behavior of the reddening in the SMC in the IR and visible (see e.g., Bouchet et al., 1984, for references).

The reddening derived for N 81 is comparable with that evaluated for the intrinsic extinction in the SMC (Caldwell and Coulson, 1985). This shows that N 81 is not affected by local extinction. Consequently, N 81 should lie on the edge of the neutral hydrogen cloud mapped by McGee and Newton (1981; see Sect. 6). The situation is completely different from that found for the H II blob in the LMC N 159, which, lying inside the molecular cloud, suffers from a strong extinction.

We are viewing N 81 projected off the center of the H I cloud, as we are looking at it with an angle. The cloud center is seen to coincide with the H II complex N 83/N 84.

The very low reddening of N 81 is confirmed by the extinction derived towards N 81 using the H I column density. From the gas/dust ratio for the SMC (Bouchet et al., 1985), we derive $E(B-V) = 0.06$ mag, which agrees well with that obtained from the optical data. Koornneef and Israel (1985) detected an excess continuum emission at 3.76 μm towards N 81. This emission should originate from the hot dust behind the visible nebula, or more precisely, behind the ionization front of the H II region moving into the H I cloud.

9. Concluding remarks

In this paper we have given a detailed picture of N 81 by studying a lot of its physical characteristics. We have classified N 81 as a Magellanic compact H II blob. Other representatives of this category of H II regions are N 159 Blob, N 160 A1 and A2 and N 11 A in the LMC (Heydari-Malayeri and Testor, 1982, 1983, 1985, 1986) and N 88 A in the SMC (Testor and Pakull, 1985). Small size, high excitation, high density and high extinction with respect to usual Magellanic H II regions have been found to be their main characteristics.

It is noteworthy that compared to the SMC blob N 88 A and the LMC N 160 A1, N 81 is neither dense nor reddened. The rms electron density in the former H II blobs amounts to about 1500 cm^{-3}, while the visual extinction reaches to 1.4 mag. For N 159 Blob the extinction rises to an even higher value. Given the fact that N 81 is a young H II region (about 2.5 10^6 years), and that at this stage of evolution the gas is expected to be mixed with dust, it is interesting that the ionized gas in this region is not at all affected by local dust. The separation between the gas and dust should not have taken place under the action of strong wind from the exciting star, because no high velocity features are present in the Hβ profile (Sect. 6).

N 81 is associated with an H I cloud of radial velocity $+167$ km s^{-1} lying at the border of the main body of the SMC with the bridge region between the SMC and LMC (McGee and Newton, 1981). The H II regions N 83 and N 84 lying at about 30′ (about 580 pc) east of N 81 are apparently associated with the main density peak of this H I cloud (3.5 10^{21} atoms cm^{-2}). This is confirmed by the observations of Testor and Lortet (1987) who give electron densities for N 83 and N 84 which tend to be higher than that for N 81.

The compact H II blob N 88 A lying at about 35′ (700 pc) west of N 83/84 is not apparently associated with the H I cloud of these H II regions. The high electron density of N 88 A implies that it should naturally be associated with an H I condensation, but there is no H I peak on the 167 km s^{-1} cloud corresponding to its position. Therefore, N 88 should be associated with the H I component of radial velocity $+134$ km s^{-1} (McGee and Newton, 1981, 1982), as it coincides with an H I peak on this component ($N_H = 1.6\ 10^{21}$ atoms cm^{-2}). This is in agreement with Testor and Pakull (1985) who, using velocity profile of N 88 A at Hα, associate N 88 A with the 134 km s^{-1} H I cloud.

It is interesting to note that N 88 A, which has the highest ionized gas density, is not associated with the highest H I density peak. Likewise, while the gas density can get higher values in the H II complexes N 83 and N 84 compared to N 81, no compact high excitation blobs like N 81 or N 88 A have been formed in these H II regions.

Copetti et al.(1985) derive ages for N 83 and N 88 which are comparable to that we obtain for N 81. Have these regions been formed simultaneously in a burst of star formation? Their belonging to two different H I clouds make this simultaneous formation quite fortuitous. On the contrary, they may really have a common origin if their formation has been triggered by, e.g., a collision between their parent H I clouds. Cloud collisions do not seem unlikely in the bridge region.

Undoubtedly, more observational data are needed in order to address these questions quantitatively.

Acknowledgements. We are indebted to Dr. M. Azzopardi for obtaining the EFOSC *U*, *B*, *V* frames of N 81. Our thanks are due to the referee Dr. R.C. Kennicutt for useful suggestions and commetns. We are grateful to Dr. L.B. Lucy for a critical reading of the manuscript.

References

Azzopardi, M.: 1981, Thèse d'Etat, Université de Toulouse
Bouchet, P., Lequeux, J., Maurice, E., Prévot, L., Prevot-Burnichon, M.L.: 1985, *Astron. Astrophys.* **149**, 330
Buzzoni, B., Delabre, B., Dekker, H., D'odorico, S., Enard, D., Focardi, P., Gustafsson, B., Reiss, R.: 1984, *Messenger* **38**, 9
Caldwell, J.A.R., Coulson, I.M.: 1985, *Monthly Notices Roy. Astron. Soc.* **212**, 879
Copetti, M.V.F., Pastoriza, M.G., Dottori, H.A.: 1985, *Astron. Astrophys.* **152**, 427
Copetti, M.V.F., Pastoriza, M.G., Dottori, H.A.: 1986, *Astron. Astrophys.* **156**, 111
Chiosi, C., Nasi, E., Sreenivasan, S.R.: 1978, *Astron. Astrophys.* **63**, 103
Conti, P.S., Garmany, C.D., Massey, P.: 1986, *Astron. J.* **92**, 48
Dennefeld, M., Stasińska, G.: 1983, *Astron. Astrophys.* **118**, 234
Dufour, R.J., Harlow, W.V.: 1977, *Astrophys. J.* **216**, 706
Dufour, R.J., Killen, R.M.: 1977, *Astrophys. J.* **211**, 68
Dufour, R.J., Shields, G.A., Talbot, R.J.: 1982, *Astrophys. J.* **252**, 461
Dufour, R.J.: 1984, in *Structure and Evolution of the Magellanic Clouds, IAU Symp.* **108**, eds. S. van den Bergh, K.S. de Boer, p. 353
Henize, K.G.: 1956, *Astrophys. J. Suppl.* **2**, 315
Henize, K.G., Westerlund, B.E.: 1963, *Astrophys. J.* **137**, 747
Feast, M.W.: 1970, *Monthly Notices Roy. Astron. Soc.* **149**, 291
Heydari-Malayeri, M., Testor, G.: 1982, *Astron. Astrophys.* **111**, L11
Heydari-Malayeri, M., Testor, G.: 1983, *Astron. Astrophys.* **118**, 116
Heydari-Malayeri, M., Testor, G.: 1985, *Astron. Astrophys.* **144**, 98

Heydari-Malayeri, M., Testor, G.: 1986, *Astron. Astrophys.* **162**, 180
Howarth, I.D.: 1983, *Monthly Notices Roy. Astron. Soc.* **203**, 301
Humphreys, R.M., McElroy, D.B.: 1984, *Astrophys. J.* **284**, 565
Koornneef, J., Israel, F.P.: 1985, *Astrophys. J.* **291**, 156
Kurucz, R.L.: 1979, *Astrophys. J. Suppl.* **40**, 1
Lequeux, J., Peimbert, M., Rayo, J.F., Serrano, A., Torres-Peimbert, S.: 1979, *Astron. Astrophys.* **80**, 155
Maeder, A.: 1981, *Astron. Astrophys.* **102**, 401
Maeder, A.: 1983, *Astron. Astrophys.* **120**, 113
Mathis, J.S.: 1982, *Astrophys. J.* **261**, 195
McCall, M.L.: 1982, Ph.D. Thesis, University of Texas
McGee, R.X., Newton, L.M.: 1981, *Proc. Astron. Soc. Australia* **4**, 189
McGee, R.X., Newton, L.M.: 1982, *Proc. Astron. Soc. Australia* **4**, 308
Mendoza, C.: 1983, in *Planetary Nebulae*, *IAU Symp.* **103**, ed. D.R. Flower, p. 143
O'Dell, C.R., Castañeda, H.O.: 1987, *Astrophys. J.* **317**, 686
Osterbrock, D.E.: 1974, *Astrophysics of Gaseous Nebulae*, Freeman: San Francisco
Panagia, N.: 1973, *Astron. J.* **78**, 929
Peimbert, M., Torres-Peimbert, S.: 1977, *Monthly Notices Roy. Astron. Soc.* **179**, 217
Pottasch, S.R.: 1984, *Planetary Nebulae*, Reidel, Dordrecht
Roy, J.-R., Arsenault, R., Joncas, G.: 1986, *Astrophys. J.* **300**, 624
Smith, M.G., Weedman, D.W.: 1973, *Astrophys. J.* **179**, 461
Stasińska, G.: 1980, *Astron. Astrophys.* **84**, 320
Testor, G., Pakull, M.: 1985, *Astron. Astrophys.* **145**, 170
Testor, G., Lortet, M.C.: 1987, *Astron. Astrophys.* **178**, 25
Tüg, H., White, N.M., Lockwood, G.W.: 1977, *Astron. Astrophys.* **61**, 679
Viallefond, F., Thuan, T.X.: 1983, *Astrophys. J.* **269**, 444
West, R.M., Schuster, H.-E.: 1982, *Astron. Astrophys. Suppl.* **49**, 577